Iraqi Journal of Computers, Communications, Control and Systems Engineering
Journal homepage: https://ijccce.uotechnology.edu.iq

A Proposed Approach to Relay-Base Station Link Design for 5G Radio Access Network

Razhan Q. Ali[1*], Jalal J. Hamad Ameen[2]

[1] Electrical Engineering Department, University of Salahaddin, Erbil, Iraq
[2] Electrical Engineering Department, University of Salahaddin, Erbil, Iraq
[1]razhan.ali@su.edu.krd, [2]jalal.hamadameen@su.edu.krd

DOI: https://doi.org/10.33103/uot.ijccce.25.1.5

HIGHLIGHTS

- The Innovative Relay-Based 5G RAN design establishes DWDM-RoF relay-assisted architecture to build stable and scalable 5G Radio Access Network (RAN) deployment.
- The fiber-connected relay mesh topology provides stable bidirectional communication through high SNR and OSNR values exceeding 50 dB.
- The network performance benefits from DWDM-RoF through efficient wavelength reuse and strong channel isolation which makes it a reliable alternative to conventional 5G RAN designs.

ARTICLE HISTORY

Received: 21/January/2025

Revised: 17/February/2025

Accepted: 01/March/2025

Available online: 30/April/2025

Keywords:
5G, Base Station,RAN,Relay,RoF.

ABSTRACT

The fast expansion of 5G technology requires new innovative approaches to resolve challenges with extensive signal degradation and constrained coverage extent as well as interference in high-frequency bands. The proposed research designs a 5G Radio Access Network (RAN) station link using relay stations that combine Dense Wavelength Division Multiplexing (DWDM) and Radio-over-Fiber (RoF) technological frameworks. The proposed system uses a mesh architectural network with 32 fiber-connected relay stations to enable efficient, scalable data transfer as an alternative to conventional star configurations. An OptiSystem simulation demonstrates that signal integrity enhancement occurs through the establishment of a bidirectional transmission medium that combines Erbium-Doped Fiber Amplifiers (EDFAs) with high-stability Continuous Wave (CW) lasers. The communication functions between uplink and downlink depend on Wavelength Division Multiplexing (WDM) multiplexers and demultiplexers to operate smoothly. The design delivers remarkable Signal-to-Noise Ratio (SNR) and Optical Signal-to-Noise Ratio (OSNR) measurements greater than 50 dB, which ensures quality signals transmit with low degradation to demonstrate stable and bidirectional communication. The system optimizes wavelength reuse while ensuring channel isolation and achieves optimum bandwidth utilization, which makes it a potential choice for future mobile networks. The research findings prove that DWDM-RoF is an effective solution to tackle critical 5G network needs through efficient, high-speed, accurate networks, which opens new paths for relay-assisted 5G development while stabilizing networks across different geographic locations.

I. INTRODUCTION

The rapid advancement of technologies like virtual reality (VR), Industry 4.0, the Internet of Everything (IoE), and 8K video streaming is bringing society closer to full connectivity. So that causes telecommunications networks to experience a massive surge in data traffic. Global mobile data consumption is expected to exceed 5,036 exabytes per month, in parallel with increasing data usage from 5GB per month in 2020 to more than 250GB per month. Experts and industry pioneers are working to innovate next-generation mobile communication technologies to meet this unmatched demand. The optimal solution lies in deploying 5G networks that are designed to connect society through three essential applications: massive machine-type communications (mMTC), enhanced mobile broadband (eMBB), and ultra-reliable low-latency communications (URLLC). As a fundamental component, eMBB plays a critical role by ensuring faster data speeds and greater network capacity to handle growing traffic loads[1].

The effectiveness of 5G fundamentally relies on enhancements in Radio Access Network (RAN) design, which play a key role in managing escalating data traffic and fulfilling the requirements of present applications [2]. Cloud Radio Access Network (C-RAN) technology is a significant advancement in 5G RAN. It consolidates baseband tasks into Baseband Unit (BBU) pools or Central Units (CUs). This streamlined method cuts down on costs, makes the best use of resources, and effectively manages a large number of remote Radio Heads (RRHs) or Radio Units (RUs), offering a solution that can grow with the needs of 5G networks [3]. Relay systems play a vital role in enhancing coverage and signal quality, especially in hard-to-reach areas like urban canyons and rural zones [4]. With the advancement in 3GPP standards, fixed and mobile relays—such as IAB (release 16), conventional repeaters (release 17), and smart repeaters (release 18)hold substantial benefits for boosting 5G network performance [5], [6], [7], [8].This study introduces an innovative relay-based station link concept for 5G Radio Access Networks, using fiber optic connections between relays. This approach uses a wired mesh topology, including Dense Wavelength Division Multiplexing (DWDM)and Radio-over-Fiber(RoF) technologies, deviating from conventional star topologies. The proposed architecture enhances flexibility, scalability, and network performance while ensuring high Signal-to-Noise Ratio (SNR) and Optical Signal-to-Noise Ratio (OSNR) for dependable communication. Difficulties like coverage restrictions and resource allocation in relay-based RAN topologies are highlighted in this study, establishing a basis for adaptive and efficient 5G communication systems that accommodate future applications.

The organization of this paper is presented as follows: Section II literature review related to the work. Section III describes the system-based methodologies employed. Section IV explains the proposed DWDM-RoF relay-base station system. Section V gives a detailed discussion of the results and a complete analysis. Section VI provides a conclusion with key findings and recommendations for future research. Finally, documents the references consulted in this study.

II. RELATED WORK

Recently, a renewed focus has been placed on relaying technology as a fundamental pillar block for the future evolution of 5G RAN. In [9], it is highlighted that UAV-based relays contribute to improving throughput by optimizing trajectory as well as power allocation in dynamic wireless networks. Another investigation [10] focused solely on RIS-assisted relay mesh networks, noting throughput gains in densely deployed urban canyons by reducing routing interference; the report also

did not examine hybrid fiber-wireless systems or latency gains. Additionally, reinforcement learning has been used to optimize relay selection in wireless sensor networks under an impulsive noise model [11]; yet, no efforts have been made to utilize it in fiber-based systems.

A follow-up study assessed wireless relay configurations in 5G networks [12], revealing improvements in capacity and latency; however, the challenges of integrating these systems with fiber optic connections remain unexamined. A Network Digital Twin framework [13] was implemented for the virtual optimization of relay systems, emphasizing wireless situations without consideration of fiber integration. Standardization initiatives [14] incorporated wireless relays with 3GPP standards, while network-controlled repeaters [15] effectively enhanced coverage and capacity; likewise, hybrid relay technologies that integrate fiber and wireless components were not considered. Research on user equipment relaying [16] explored post-5G but maintained a focus persisted on wireless relays.

Hybrid relay systems, which integrate fiber and wireless technology, have garnered little attention. A review on relay-assisted optical wireless communications [17] emphasized the benefits of hybrid designs for low latency and higher reliability. Although Cooperative relaying in Rayleigh fading channels [18] demonstrated promise for 5G networks in urban regions. Nevertheless, the key aspects, such as enhancing Service quality and smooth transitions in hybrid relaying situations remain unexplored.

III. SYSTEM BASED METHOLOGY

A. Optical Fiber Communication System

RoF is a system that works by integrating fiber optic networks for transmitting radio frequency (RF) signals from a central hub to distant antenna units. This technology combines optical and microwave systems to provide a dependable solution that enhances network capabilities and mobility features at cost-effective rates [19]. As shown In *Fig. 1,* the RoF system requires three essential elements that perform unique functions, starting with the central station (CS) and continuing with the optical fiber network and finishing with the base station (BS). The central station acts as the transmitter, monitoring signal formation and modulation; the base station operates as the receiver, receiving and processing signals from the fiber optic network. The data source working with the laser operates at the CS as a transmitter to transform electrical signals into optical signals. The base station collects signals through fiber optic transmission. The fiber optic network employs remote nodes to enhance and dissemi

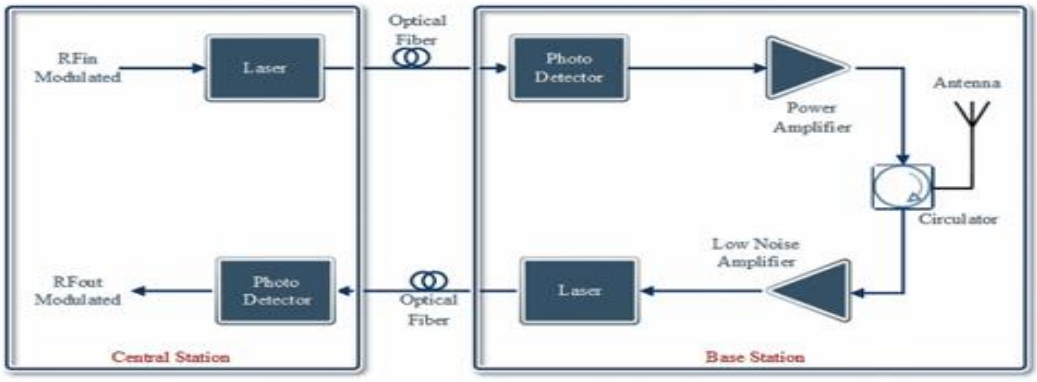

FIG. 1. GENERAL STRUCTURE OF FIBER OPTIC COMMUNICATION SYSTEM [19].

At the base station, a compact antenna device, commonly known as a remote antenna, converts the optical signal back into an electrical signal for the end user. Through the base station, radio signals received from end users get converted into optical signals before transmission to the central station through the fiber optic network [19].

B. Wavelength Division Multiplexing

The 5G networking element WDM plays a vital role by combining optical signals through separate wavelengths for extended data transmission. The signals reach separate channels upon reception which results in substantial capacity growth for the system. DWDM emerges as the most efficient WDM technology because it enables increased transmission capacity together with extended distances and extensive wavelength spectrum use.

The combination of RoF technologies with DWDM in 5G communication networks enables faster data rates and improved bandwidth performance, which establishes them as the optimal solution for next-generation networks [20]. *Fig. 2*, illustrates the fundamental concept of WDM technology, showing its ability to manage several signals simultaneously.

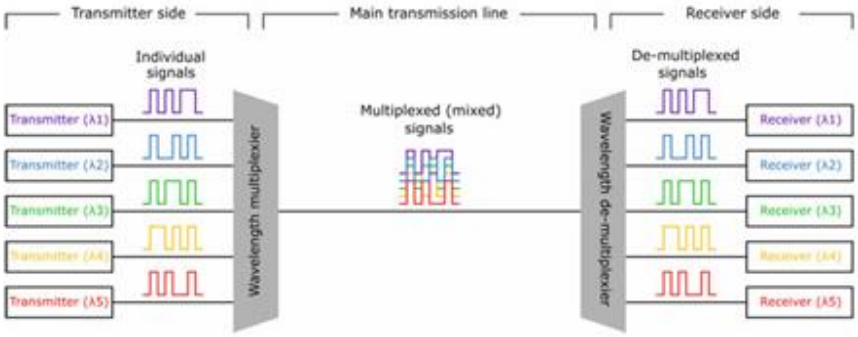

FIG. 2. WDM-BASED TECHNOLOGY BASIC DIAGRAM [20].

IV. PROPOSED DWDM-RoF RELAY-BASE STATION SYSTEM

The system design employs 32 channels of 32 relay stations connected through WDM fiber optics to 32 remote stations at the receiving end, as shown in *Fig. 3*, for 7 relays. The proposed configuration was simulated using OptiSystem software V22, a well-established tool renowned for its efficacy in designing, testing, and modelling diverse fiber optic systems. The software system delivers precise performance evaluation capabilities for system testing under various circumstances. *Fig. 4* displays the 32-channel DWDM system, demonstrating the relay-based fiber link architecture. This design

facilitates seamless communication between relay stations and distant stations, leveraging the efficacy of WDM technology for fast and low-loss data transmission over several channels.

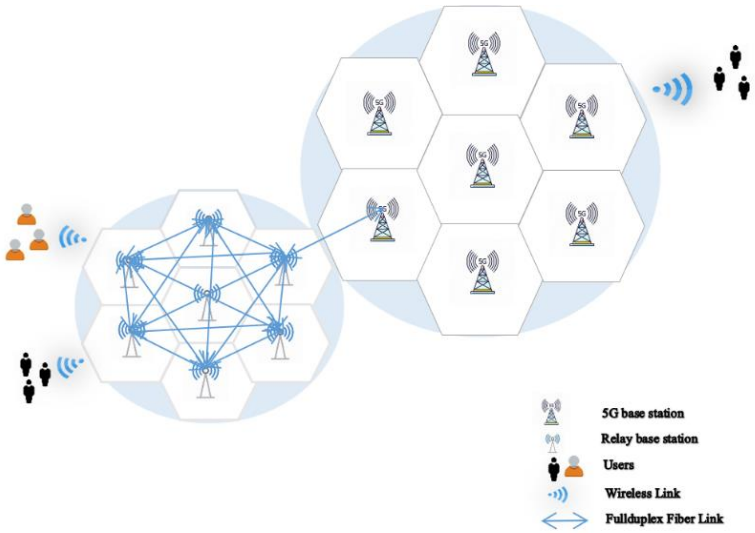

FIG. 3. RELAY BASE STATION SCENARIO.

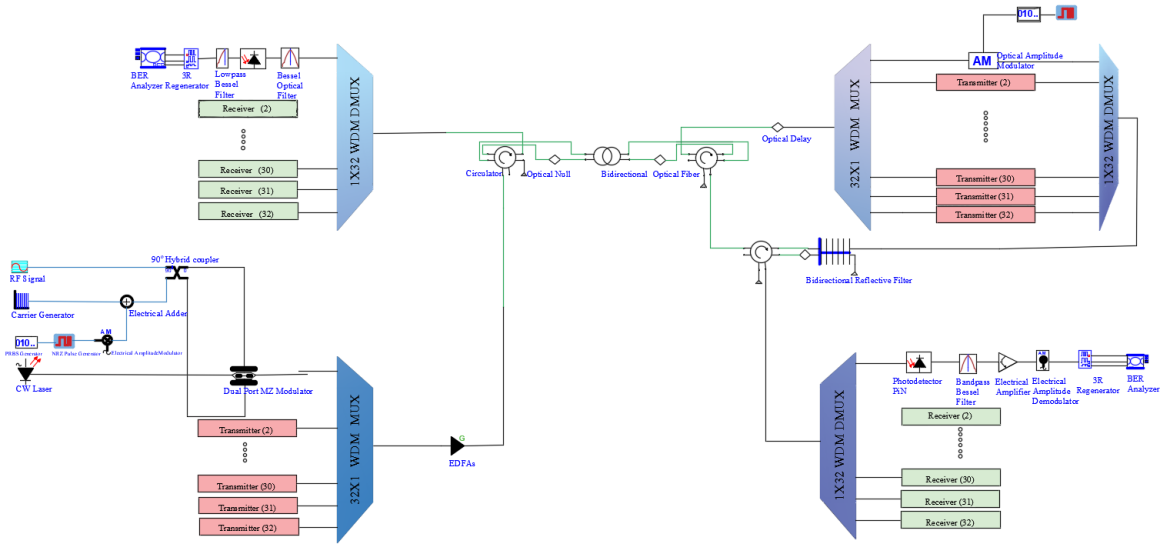

FIG. 4. SYSTEM DESIGN BLOCK DIAGRAM.

A. Transmitter Part

The system integrates electrical and optical components to facilitate efficient digital data transfer via an optical fiber link, which consists of 32 channels. Every wavelength-operated channel connects to an associated relay device. The initial channel operates at 193.1 THz with a 1 MHz linewidth, but other channels maintain a 0.8 nm separation for low-loss transmission and higher user density and increased data rates. Each channel sustains an input power of 6 dBm. The baseband signal emerges through non-return-to-zero (NRZ) pulses, which result from processing binary data by a pseudo-random bit generator. An electrical adder subsequently combines the signal with a carrier signal from a carrier

generator, and an electrical amplitude modulator (AM) operating at a frequency of 3.5 GHz adjusts the signal amplitude according to the input data.

The modulated signal is fed into a Continuous Wave (CW) laser to generate an optical carrier wave. A 90° hybrid coupler applies a phase shift, enabling subcarrier multiplexing. The output proceeds to a dual-port lithium niobate ($LiNbO_2$) Mach-Zehnder modulator (MZM) for additional processing that transforms electrical signals into optical signals. A WDM multiplexer with an 80 GHz bandwidth integrates the optical signals from all 32 channels into a unified transmission. This setup facilitates rapid, high-density, and low-loss communication across the optical fiber link.as shown in *Fig. 5* below.

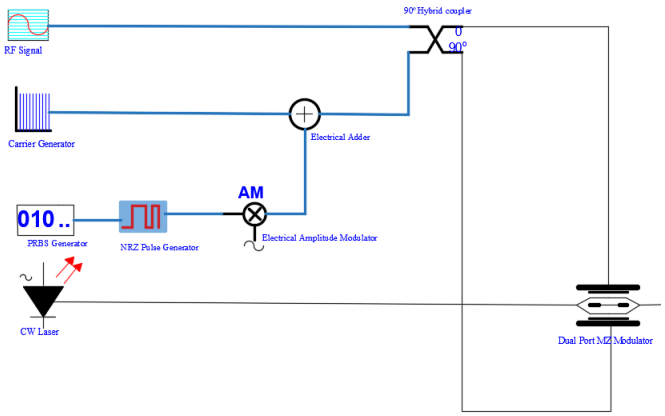

FIG. 5. INTERNAL STRUCTURE OF TRANSMITTER.

B. Transmission Medium Part

Erbium-Doped Fiber Amplifiers (EDFAs), as essential components of optical communication systems, enhance signal strength across multiple channels simultaneously, function to amplify signals effectively within the 1550 nm wavelength range, optimal for optical signal amplification, and also optical interference of the system between downlink and uplink signals minimized by utilizing a bidirectional circulator, ensuring smooth and continuous data transmission. Furthermore, the signal transmission reliability and system performance can be improved by using a 1-kilometer-long optical fiber to simulate relay distances allows for dependable and continuous signal transmission, enhancing the system's resilience and efficiency as shown in *Fig. 6* below.

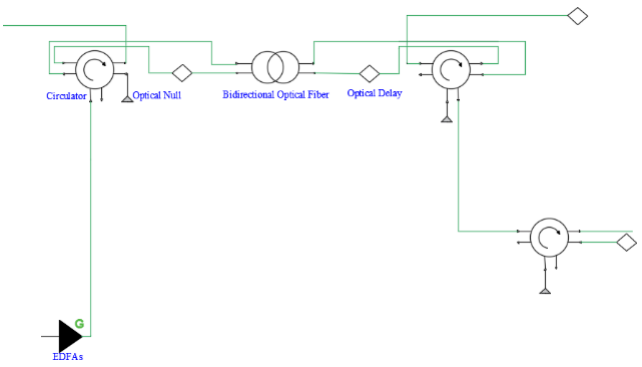

FIG. 6. FIBER LINK WITH MEDIUM COMPONENTS.

TABLE I. THE EDFAS SELECTED PARAMETERS.

EDFAs Parameters	Parameter Value
Gain	20 dB
Noise Figure	4 dB
Operation Mode	Power control
Power	15 dBm
Saturation Power	10 dBm
Include Noise	Yes

TABLE II. THE FIBER LINK PARAMETERS.

Bidirectional Optical Fiber Parameters	Parameter Value
Length	1km
Reference Wavelength	1550nm
Dispersion	17 Ps/nm/km
Dispersion Slop	0.07 Ps/nm^2/km

C. Reseiver Part

The WDM demultiplexer equipped with 80 GHz bandwidth splits the received signal before it directs the data to receivers at the endpoint. The bidirectional reflective filter functions as the main component of this operation by letting some signal pass through as it reflects the rest of the data-carrying signal for continued demodulation. The PIN photodiode converts the reflected signal which moves through a band-pass filter before the signal reaches the signal analyzer at downlink.

The portion of the signal sent via the bidirectional reflective filter is re-modulated by an amplitude modulator driven by a 20 Gbps baseband signal. A WDM MUX with an 80 GHz bandwidth merges the modulated signals from all channels and is retransmitted as an uplink signal to the transmitter side. At the transmitter, a WDM de-multiplexer with a bandwidth of approximately 80 GHz demultiplexes the uplink signal, and then the demultiplexed signal is subsequently converted to electrical signal using a PIN photodiode and refined through a Bessel filter for conclusive analysis, as shown in *Fig. 7* below and indicated in Table III.

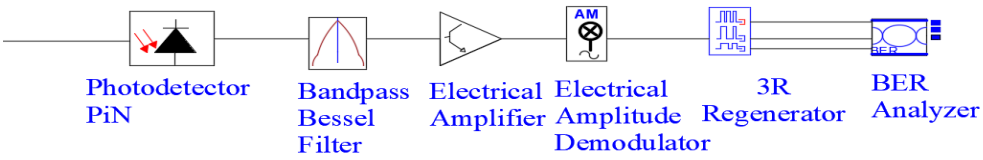

FIG. 7. SYSTEM DOWNLINK RECEIVER PART.

TABLE III. RECEIVER PART PARAMETERS VALUE FOR BOTH UPLINK AND DOWNLINK.

Downlink Receiver		Uplink Receiver	
Photodetector	values	Bandpass Bessel filter	values
Responsivity	1A/W	Frequency*	193.1 THz
Dark current	10nA	Bandwidth	12 GHz
Bandpass Bessel filter	values	Photodetector	values
Frequency	3.5 GHz	Responsivity	1A/W
Bandwidth	1 GHz	Dark current	10nA
Electrical amplifier	value	Lowpass Bessel filter	value
Gain	20dB	Cut off frequency	0.72*Bit rate
AM demodulator	values	3R Regenerator	value
Frequency	3.5GHz	Reference Bit rate	20Gbps
Cut off frequency	0.72*Bit rate		

* This frequency changes according to each channel.

V. RESULTS AND DISCUSSION

Table IV outlines the wavelengths assigned to each of the 32 WDM channels, ranging from 193.1 THz to 196.2 THz. Each channel is allocated a distinct frequency.

TABLE IV. THE UTILIZED WAVELENGTHS.

Channel Number	Wavelength	Channel Number	Wavelength
Ch 1	193.1 THz	**Ch 17**	194.7 THz
Ch 2	193.2 THz	**Ch 18**	194.8 THz
Ch 3	193.3 THz	**Ch 19**	194.9 THz
Ch 4	193.4 THz	**Ch 20**	195.0 THz
Ch 5	193.5 THz	**Ch 21**	195.1 THz
Ch 6	193.6 THz	**Ch 22**	195.2 THz
Ch 7	193.7 THz	**Ch 23**	195.3 THz
Ch 8	193.8 THz	**Ch 24**	195.4 THz
Ch 9	193.9 THz	**Ch 25**	195.5 THz
Ch 10	194.0 THz	**Ch 26**	195.6 THz
Ch 11	194.1 THz	**Ch 27**	195.7 THz
Ch 12	194.2THz	**Ch 28**	195.8 THz
Ch 13	194.3 THz	**Ch 29**	195.9 THz
Ch 14	194.4 THz	**Ch 30**	196.0 THz
Ch 15	194.5 THz	**Ch 31**	196.1 THz
Ch 16	194.6 THz	**Ch 32**	196.2 THz

The RF signal generated by the sine wave generator, as demonstrated in *Fig. 8* (A), features a pure single-frequency spectrum, offering exceptional spectral clarity that ensures minimal disruption and facilitates effective subcarrier modulation. The hybrid coupler applies a 90° phase shift, producing orthogonal signals necessary for subcarrier multiplexing, as illustrated in *Fig. 8* (B). Amplitude variations indicate strengthened modulation.

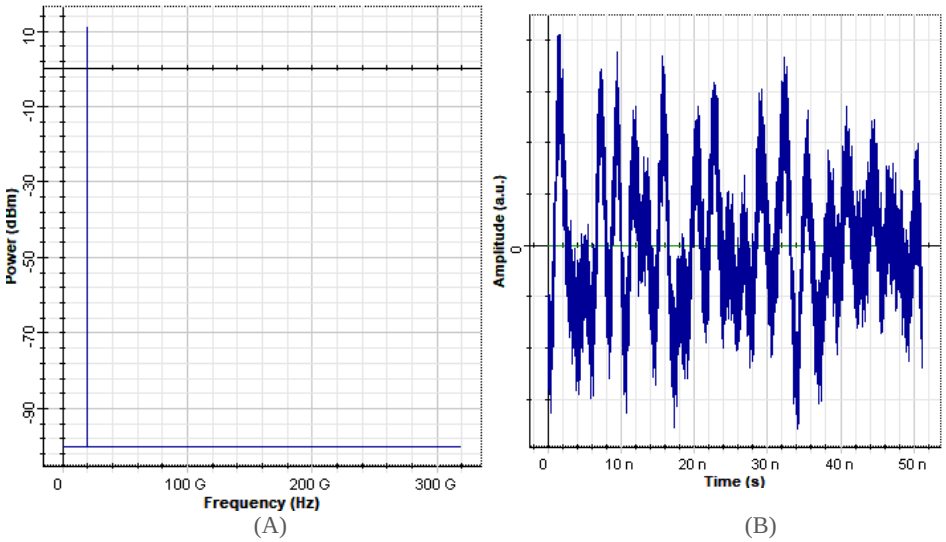

(A) (B)

FIG. 8. (A) RADIO FREQUENCY SIGNAL, (B) RADIO FREQUENCY AFTER 90-DEGREE PHASE SHIFT.

Fig. 9 (A) ,illustrates the binary signal from the NRZ pulse generator, preserving data integrity, and then, as shown in *Fig. 9* (B), the NRZ data integrates with a carrier signal of amplitude modulation, ensuring compatibility for optical conversion and reliable transmission.

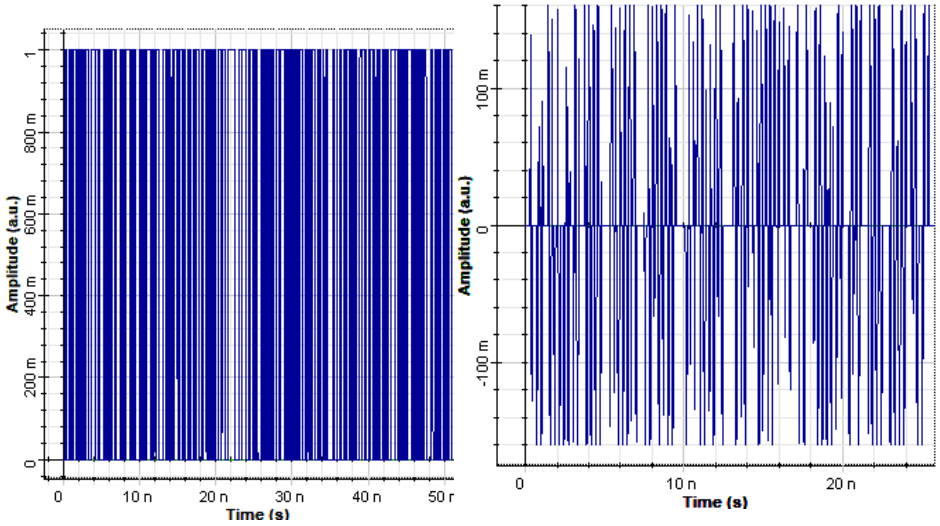

(A) (B)

FIG. 9. (A) DIGITAL DATA, (B) MODULATED SIGNAL AFTER AM MODULATOR.

The carrier generator produces a stable sinusoidal signal for modulation, which is combined with an NRZ-AM modulated signal by an electrical adder. A composite waveform is formed that encodes binary information. As the signal moves through the 0° coupler, the phase and amplitude remain as is, ensuring it is ready for further modulation and transmission, as demonstrated in *Fig. 10.* The CW laser's output spectrum, depicted in *Fig. 11*, shows a sharp peak at 193.1 THz, indicating stable and precise optical carrier generation. The stability level is crucial for accurate modulation and reliable signal transmission within optical networks.

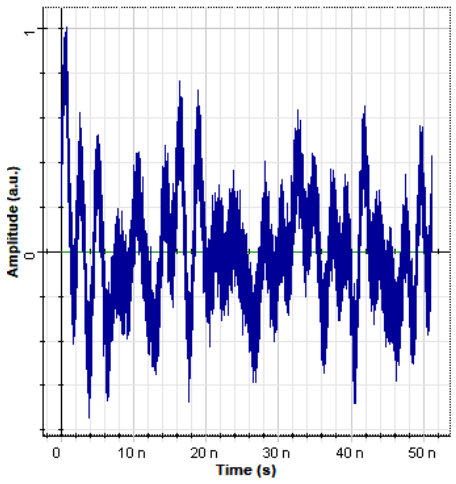

FIG. 10. CARRIER GENERATOR AFTER 0-DEGREE COUPLER.

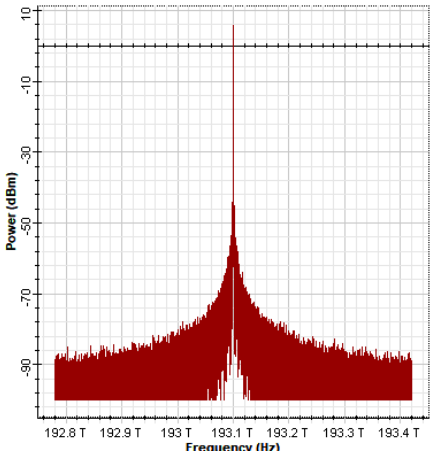

FIG. 11. CW LASER SPECTRUM.

Fig. 12 shows MZM outputs in a system of 32 channels, which present only for four channels: 193.1 THz, 194 THz, 195 THz, and 196 THz, respectively, that exhibit distinct peaks, signifying stable and robust optical carriers. Well-balanced power distribution and low noise of the system emphasize optimal maintenance of excellent signal integrity and less distortion.

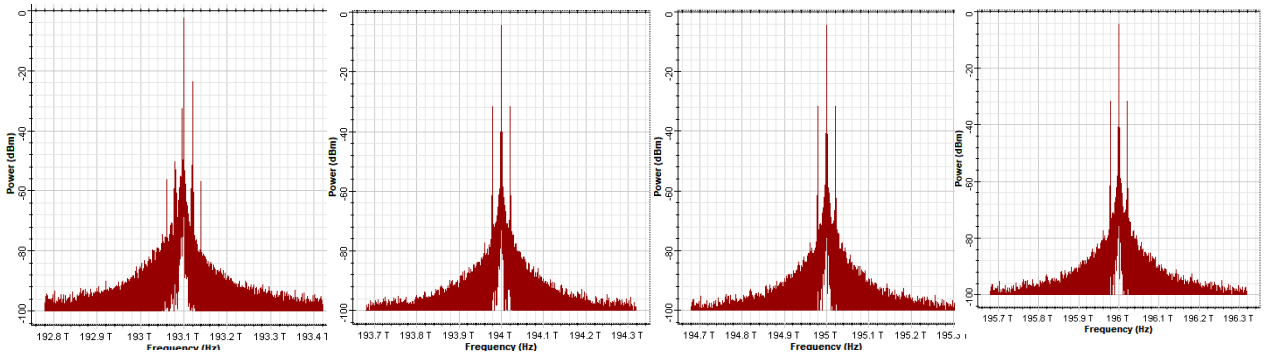

(A) (B) (C) (D)

FIG.12. A-D OUTPUT SPECTRUM OF MZM FOR THE FREQUENCY 193.1THZ, 194THZ, 195THZ AND 196THZ RESPECTIVELY.

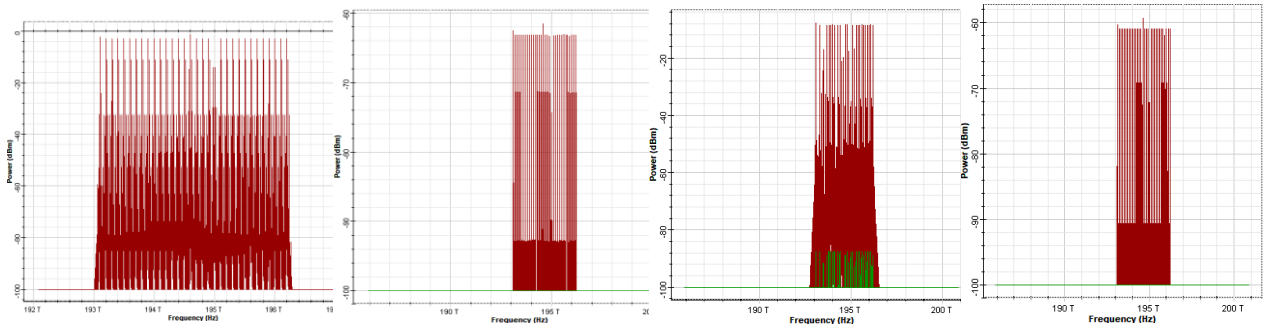

(A) (B) (C) (D)

FIG. 13. A-D FREQUENCY SPECTRA OF WDM MUX FOR THE DOWNLINK AND UPLINK RESPECTIVELY.

The system's proficiency in handling bidirectional communication is illustrated by the frequency spectra for the uplink and downlink components in *Fig. 13*. Effective WDMMUX channel allocation is highlighted by well-defined peaks in the uplink and downlink transmitter spectra, while the receiver spectra confirm reliable transmission and reception with minimal distortion but with little interference and precise channel separation.

Figs. 14 and *15* distinctly display the spectra of four DEMUX channels from both the downlink and uplink, with clear peaks at their respective frequencies. The clear separation between the channels and the uniform power levels across the spectra demonstrate effective channel isolation that underscores the dependable functionality of the WDM system, reinforcing the reliability of the WDM system in supporting precise bidirectional communication with little interference or crosstalk among channels.

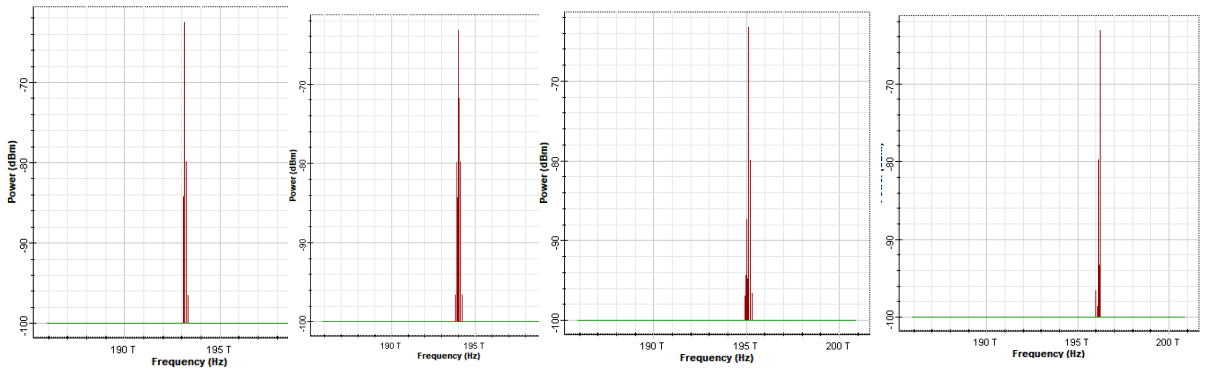

(A) (B) (C) (D)

FIG. 14. A-D DOWNLINK DEMUX OUTPUT FOR FREQUENCY 193.1, 194.195, 196THZ RESPECTIVELY.

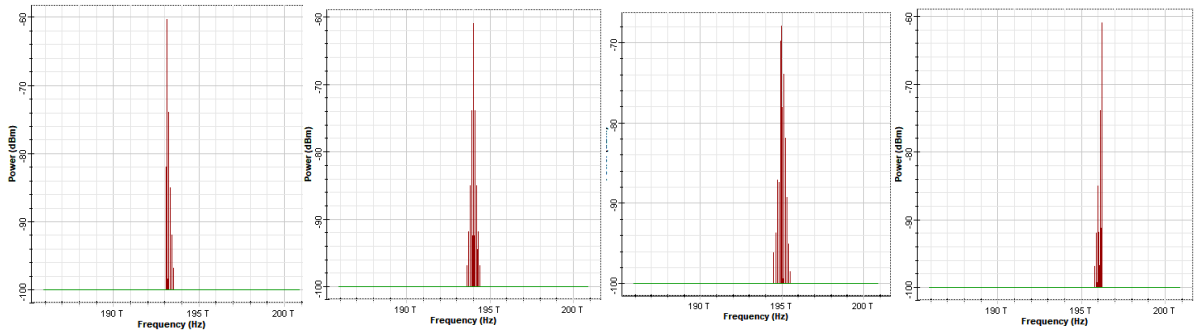

(A) (B) (C) (D)

FIG.15. A-D UPLINK DEMUX OUTPUT FOR FREQUENCY 193.1, 194.195, 196THZ RESPECTIVELY.

Table V shows the performance characteristics of the uplink WDM system at both the transmitter and receiver ends. The transmitter side demonstrates uniform signal strength. Across channels with low noise power, obtain elevated SNR and OSNR values (exceeding 50 dB), signifying pristine signal creation and the noise power experiences a slight rise due to transmission effects on the receiver side.

The downlink WDM system's performance at both the transmitter and receiver sides is analyzed in Table VI. Signal power is about -2.69 dBm per channel, with noise power of -35 dBm, leading to SNR values ranging from 28 to 33 dB. OSNR values range from 31 to 35 dB at the transmitter side, which reflects adequate optical signal quality; nevertheless, further noise mitigation could optimize performance. At the receiver, it experiences a slight reduction, somewhat from -4.6 dBm to -6.8 dBm, as a result of anticipated transmission attenuation. The noise power is from -55 to -57 dBm at the receiver, maintaining SNR values above 50 dB and an average OSNR of 52 dB, resulting in excellent signal integrity after transmission. While the system demonstrates strong performance, further noise reduction at the transmitter could enhance proper alignment with the receiver's robust metrics.

TABLE V. UPLINK TRANSMITTER AND RECEIVER SIDE OF WDM ANALYZERS METRICS RESPECTIVELY.

WDM Analyzer

Frequency (THz)	Signal Power (dBm)	Noise Power (dBm)	SNR (dB)	Noise Power: 0.1nm (dBm)	OSNR (dB)
193.1	-6.1019996	-57.374254	51.272254	-59.415454	53.313454
193.2	-46.582963	-100	53.417037	-100	53.417037
193.3	-6.6980875	-57.4271	50.729013	-59.4683	52.770213
193.4	-30.553119	-81.563079	51.00996	-83.604279	53.05116
193.5	-10.351615	-61.56177	51.210155	-63.60297	53.251355
193.6	-30.765809	-81.423082	50.657273	-83.464282	52.698473
193.7	-6.7246518	-58.771856	52.047204	-60.813056	54.088404
193.8	-6.7530503	-57.41588	50.66283	-59.45708	52.70403
193.9	-6.7479603	-57.428784	50.680824	-59.469984	52.722024
194	-6.7844141	-57.606045	50.821631	-59.647245	52.862831
194.1	-6.7339307	-57.351818	50.617887	-59.393018	52.659087
194.2	-47.902555	-100	52.097445	-100	52.097445
194.3	-6.730219	-57.404697	50.674478	-59.445897	52.715678
194.4	-6.7576385	-57.417601	50.659962	-59.458801	52.701162
194.5	-19.356912	-70.75022	51.393308	-72.79142	53.434508
194.6	-17.872672	-70.289979	52.417306	-72.331179	54.458506
194.7	-6.7076869	-58.749495	52.041808	-60.790695	54.083008
194.8	-6.7027979	-57.393537	50.690739	-59.434736	52.731939
194.9	-10.234655	-61.359692	51.125037	-63.400892	53.166237
195	-21.430691	-57.574969	36.144278	-59.616169	38.185478
195.1	-6.8149374	-57.329499	50.514562	-59.370699	52.555762
195.2	-10.333719	-62.691602	52.357882	-64.732801	54.399082
195.3	-6.7649105	-57.382407	50.617496	-59.423607	52.658096
195.4	-6.7564559	-57.395309	50.638853	-59.436508	52.680053
195.5	-6.7645825	-57.563844	50.799261	-59.605044	52.840461
195.6	-6.8161261	-57.318381	50.502255	-59.359581	52.543455
195.7	-6.7521291	-58.727245	51.975116	-60.768444	54.016315
195.8	-6.7450648	-57.371303	50.626238	-59.412503	52.667438
195.9	-6.7129153	-57.384207	50.671292	-59.425407	52.712492
196	-6.7446973	-57.552749	50.808052	-59.593949	52.849252
196.1	-6.7167885	-57.307294	50.590505	-59.348494	52.631705
196.2	-6.7420271	-58.71617	51.974143	-60.75737	54.015343

WDM Analyzer

Frequency (THz)	Signal Power (dBm)	Noise Power (dBm)	SNR (dB)	Noise Power: 0.1nm (dBm)	OSNR (dB)
193.1	-8.3300824	-59.594206	51.264123	-61.635406	53.305323
193.2	-49.659944	-100	50.340056	-100	50.340056
193.3	-8.9117339	-59.647051	50.735317	-61.688251	52.776517
193.4	-33.187364	-83.770369	50.583005	-85.811569	52.624205
193.5	-12.550183	-63.781643	51.23146	-65.822843	53.27266
193.6	-33.053499	-83.63076	50.577261	-85.671959	52.61846
193.7	-8.9140119	-60.991789	52.077777	-63.032989	54.118977
193.8	-8.9445889	-59.635831	50.691242	-61.677031	52.732442
193.9	-8.951447	-59.646735	50.695288	-61.688935	52.738488
194	-8.9882158	-59.825994	50.837778	-61.867194	52.878978
194.1	-8.9475424	-59.571769	50.624227	-61.612969	52.665427
194.2	-51.488927	-100	48.511073	-100	48.511073
194.3	-8.9526371	-59.624648	50.672011	-61.665848	52.713211
194.4	-8.9704949	-59.637552	50.667057	-61.678751	52.708257
194.5	-21.641153	-72.969159	51.328006	-75.010358	53.369206
194.6	-20.079879	-72.509023	52.429144	-74.550223	54.470344
194.7	-8.8950595	-60.969428	52.074369	-63.010628	54.115569
194.8	-8.9032843	-59.613487	50.710203	-61.654687	52.751403
194.9	-12.437992	-63.57957	51.141577	-65.620769	53.182777
195	-23.662072	-59.794918	36.132846	-61.836118	38.174046
195.1	-9.0487982	-59.549451	50.500653	-61.590651	52.541852
195.2	-12.527959	-64.911435	52.383476	-66.952635	54.424676
195.3	-8.961787	-59.602358	50.640571	-61.643558	52.681771
195.4	-8.9816204	-59.615259	50.633639	-61.656459	52.674839
195.5	-8.9895993	-59.783792	50.794193	-61.824992	52.835393
195.6	-9.0106348	-59.538333	50.527698	-61.579533	52.568898
195.7	-8.9461543	-60.947178	52.001023	-62.988377	54.042223
195.8	-8.9678307	-59.591254	50.623423	-61.632454	52.664623
195.9	-8.9324885	-59.604158	50.671669	-61.645358	52.712869
196	-8.963828	-59.772698	50.80887	-61.813898	52.85007
196.1	-8.9279439	-59.527245	50.599301	-61.568445	52.640501
196.2	-8.969928	-60.936103	51.966175	-62.977303	54.007375

TABLE VI. DOWNLINK TRANSMITTER AND RECEIVER SIDE OF WDM ANALYZERS METRICS RESPECTIVELY.

WDM Analyzer

Frequency (THz)	Signal Power (dBm)	Noise Power (dBm)	SNR (dB)	Noise Power: 0.1nm (dBm)	OSNR (dB)
193.1	-2.0390252	-35.343209	33.304184	-37.384409	35.345383
193.2	-2.6907408	-35.343209	32.652468	-37.384409	34.693668
193.3	-2.6907394	-35.343209	32.652469	-37.384409	34.693669
193.4	-2.6907401	-35.343209	32.652469	-37.384409	34.693669
193.5	-2.6907403	-35.343209	32.652468	-37.384409	34.693668
193.6	-2.6907403	-35.343203	32.652463	-37.384403	34.693863
193.7	-2.6907403	-35.304619	32.613879	-37.345819	34.655078
193.8	-2.6907403	-32.306515	29.615775	-34.347715	31.656975
193.9	-2.6907403	-32.305398	29.614658	-34.346598	31.655858
194	-2.6907403	-31.432796	28.742056	-33.473996	30.783256
194.1	-2.6907403	-32.307068	29.616327	-34.348268	31.657527
194.2	-2.6907403	-32.307603	29.616863	-34.348803	31.658062
194.3	-2.6907406	-32.301358	29.610618	-34.342558	31.651817
194.4	-2.6907409	-30.599532	27.908791	-32.640731	29.949991
194.5	-2.6907464	-32.307206	29.61646	-34.348406	31.65766
194.6	-1.0916151	-32.307044	31.215429	-34.348244	33.256629
194.7	-2.6907607	-32.307014	29.616253	-34.348214	31.657453
194.8	-2.6907482	-32.306895	29.616147	-34.348095	31.657347
194.9	-2.6932173	-32.304726	29.611509	-34.345926	31.652709
195	-17.609073	-32.294217	14.685145	-34.335417	16.726345
195.1	-2.6907543	-32.307613	29.616859	-34.348813	31.658059
195.2	-2.6907381	-31.423957	28.733219	-33.465156	30.774418
195.3	-2.690738	-32.272373	29.581635	-34.313573	31.622835
195.4	-2.690741	-32.307055	29.616314	-34.348255	31.657514
195.5	-2.6907934	-32.298364	29.60757	-34.339563	31.64877
195.6	-2.695368	-30.613299	27.917931	-32.654499	29.959131
195.7	-2.6906964	-35.284054	32.593358	-37.325254	34.634558
195.8	-2.6906797	-35.291894	32.601214	-37.333094	34.642414
195.9	-2.6945803	-35.291729	32.597149	-37.332929	34.638349
196	-2.6907756	-35.29175	32.600975	-37.33295	34.642174
196.1	-2.6907418	-35.292079	32.601337	-37.333278	34.642537
196.2	-2.6907262	-35.253547	32.562821	-37.294747	34.60402

WDM Analyzer

Frequency (THz)	Signal Power (dBm)	Noise Power (dBm)	SNR (dB)	Noise Power: 0.1nm (dBm)	OSNR (dB)
193.1	-6.2218031	-57.306199	51.084396	-59.347399	53.125596
193.2	-6.4835793	-56.899646	50.415066	-58.939845	52.456266
193.3	-6.0587622	-56.526165	50.467402	-58.567364	52.508602
193.4	-5.7551021	-56.183671	50.428569	-58.224871	52.469769
193.5	-5.468543	-55.882681	50.414138	-57.923881	52.455338
193.6	-5.1734169	-55.6005	50.427083	-57.6417	52.468283
193.7	-4.9183592	-55.352662	50.434303	-57.393062	52.475502
193.8	-4.6893181	-55.132198	50.44288	-57.173398	52.48408
193.9	-4.5166283	-54.937359	50.42073	-56.978558	52.46193
194	-4.3419547	-54.77213	50.430176	-56.81333	52.471375
194.1	-4.1980049	-54.625589	50.427504	-56.666789	52.468704
194.2	-4.1114611	-54.506199	50.394738	-56.547399	52.435938
194.3	-3.9806711	-54.410486	50.429815	-56.451686	52.471015
194.4	-3.9317908	-54.339823	50.408032	-56.381022	52.449232
194.5	-3.8547743	-54.291771	50.436996	-56.332971	52.478196
194.6	-2.2273517	-54.26535	52.037998	-56.30655	54.079198
194.7	-3.8168661	-54.262539	50.445678	-56.303738	52.486877
194.8	-3.8300208	-54.282617	50.452596	-56.323817	52.493796
194.9	-3.9304164	-54.329614	50.399197	-56.370814	52.440397
195	-19.470083	-54.394702	34.924619	-56.435902	36.965819
195.1	-4.1160157	-54.486337	50.370321	-56.527537	52.411521
195.2	-4.2202521	-54.600099	50.379846	-56.641298	52.421046
195.3	-4.3363128	-54.73797	50.401657	-56.77917	52.442857
195.4	-4.4934999	-54.906818	50.413318	-56.948018	52.454518
195.5	-4.6984699	-55.091304	50.392834	-57.132503	52.434033
195.6	-4.8911349	-55.310097	50.418962	-57.351296	52.460161
195.7	-5.1405578	-55.552286	50.411728	-57.593485	52.452928
195.8	-5.4174689	-55.823126	50.405657	-57.864325	52.446857
195.9	-5.711846	-56.133142	50.421296	-58.174342	52.462496
196	-6.0485541	-56.459587	50.411033	-58.500787	52.452233
196.1	-6.3894029	-56.833288	50.443885	-58.874488	52.485085
196.2	-6.8025133	-57.235151	50.432637	-59.27635	52.473837

VI. CONCLUSION

By implementing DWDM and RoF technologies, the proposed relay-based station architecture adeptly addresses critical obstacles in 5G RAN. With the integration of optical technology to sustain continuous SNR and OSNR values exceeding 50 dB over 32 channels, delivering high-quality signal transmission with minimal degradation and clear spectral peaks, efficient reuse of wavelengths, and strong channel separation in the MUX and DEMUX outputs shows it can communicate in both directions with little interference. EDFAs with continuous-wave lasers improve system performance by maintaining dependable optical signal amplification and lowering power loss, thereby facilitating high-speed data transmission over extended distances. The relay architecture effectively provides scalability for increasing network requirements in high-density user traffic. These attributes position the system as a reinforced foundation for enhancing 5G coverage and performance, particularly in high-frequency bands where route loss and interference remain key challenges, and systems with the ability to maintain low-noise power and consistent transmission in both downlink and uplink contexts underscore and prove its dependability and efficiency.

CONFLICT OF INTEREST

Conflict of Interest the authors confirm that no conflicts of interest exist regarding this paper's publication. Salahaddin University-Erbil acknowledges its support for this research through funding for its implementation.

ACKNOWLEDGMENT

I would like to express my utmost appreciation to Salahaddin University-Erbil for their endowed financial support and funding, which made the research possible, and their assistance was valuable in pursuing and completing this study. I also extend my sincere appreciation to my supervisor, Assist. Prof. Dr. Jalal, for this guidance and encouragement.

REFERENCES

[1] A. Fayad, T. Cinkler, J. Rak, and M. Jha, "Design of Cost-Efficient Optical Fronthaul for 5G/6G Networks: An Optimization Perspective," Sensors (Basel), vol. 22, no. 23, Dec 1 2022, doi: 10.3390/s22239394.

[2] H. Hamdoun, M. Hamid, S. Amin, and H. Dafallah, "5G RAN: Key Radio Technologies and Hardware Implementation Challenges," in Optical and Wireless Convergence for 5G Networks, A. M. Abdalla, J. Rodriguez,I. Elfergani, and A. Teixeira, Eds. Hoboken, NJ: Wiley, 2020, pp. 123–136.

[3] R. Guerra-Gómez, "Radio Access Network Optimization with Proactive Resource Management for 5G and Beyond", Ph.D. dissertation, Signal Theory and Communications Dept., Universitat Politècnica de Catalunya, Barcelona, Spain, Jan. 2023.

[4] A. BenMimoune and M. Kadoch, "Relay Technology for 5G Networks and IoT Applications," in Internet of Things: Novel Advances and Envisioned Applications, D. Acharjya and M. Geetha, Eds., Studies in Big Data, vol. 25, Cham: Springer, 2017. doi: 10.1007/978-3-319-53472-5_1.

[5] 3GPP, "Study on Integrated Access and Backhaul (Release 16)," 3GPP TR 38.874, V16.0.0, Dec. 2018.

[6] 3GPP, "NR Repeater Radio Transmission and Reception (Release-17)," 3GPP TS 38.106, V17.6.0, Sep. 2023.

[7] 3GPP, "Study on NR Network-Controlled Repeaters (Release 18)," 3GPP TR 38.867, V18.0.0, Sep. 2022.

[8] 3GPP, "Proximity based Services (ProSe) in the 5G System (5GS) (Release-18)," 3GPP TS 23.304, V18.3.0, Sep. 2023.

[9] S. Nasrollahi and S. M. Mirrezaei, "Toward UAV-based communication: improving throughput by optimum trajectory and power allocation," EURASIP Journal on Wireless Communications and Networking, vol. 2022, no. 1, 2022, doi: 10.1186/s13638-022-02087-6.

[10] C. V. Phung, A. Drummond and A. Jukan, "Maximizing Throughput with Routing Interference Avoidance in RIS-Assisted Relay Mesh Networks," 2024 47th MIPRO ICT and Electronics Convention (MIPRO), Opatija, Croatia,2024, pp. 736-741, doi: 10.1109/MIPRO60963.2024.10569578.

[11] H. Barka, M. S. Alam, G. Kaddoum, M. Au and B. L. Agba, "RL-Based Relay Selection for Cooperative WSNs in the Presence of Bursty Impulsive Noise," 2024 IEEE Wireless Communications and Networking Conference (WCNC), Dubai, United Arab Emirates, 2024, pp. 1-6, doi: 10.1109/WCNC57260.2024.10570780.

[12] J. Luo, A. Sampath, N. Abedini and T. Luo, "Performance study of various relay nodes in 5G wireless network," arXiv preprint, arXiv:2407.20089, 2024.

[13] F. F. Pons, "Exploring Relay Technology for 5G and Beyond Systems through the use of a Network Digital Twin," Master Thesis, Escola T`ecnica d'Enginyeria de Telecomunicaci´o de Barcelona, Universitat Polit`ecnica de Catalunya, 2023.

[14] S. Narayanan et al., "Relaying solutions for 5G-IoT applications: A 3GPP perspective," IEEE Communications Standards Magazine, vol. 8, no. 2, pp. 28–35, 2024, doi: 10.1109/MCOMSTD.0005.2300019.

[15] F. Carvalho et al., "Network-controlled repeater--An introduction," arXiv preprint, arXiv:2403.09601, 2024.

[16] J. Pérez-Romero, O. Sallent, and O. Ruiz, "On exploiting user equipment relaying capabilities in beyond 5G networks: Opportunities, challenges, and road map," IEEE Vehicular Technology Magazine, 2024.

[17] W. Liu, J. Ding, J. Zheng, X. Chen and C. -L. I, "Relay-Assisted Technology in Optical Wireless Communications: A Survey," in IEEE Access, vol. 8, pp. 194384-194409, 2020, doi: 10.1109/ACCESS.2020.3031288.

[18] L. Teng, W. An, C. Dong, X. Qin and X. Xu, "Performance Analysis of MDMA-Based Cooperative MRC Green Networks with Relays in Dissimilar Rayleigh Fading Channels," 2024 IEEE International Conference on Communications Workshops (ICC Workshops), Denver, CO, USA, 2024, pp. 57-62, doi: 10.1109/ICCWorkshops59551.2024.10615474.

[19] M. Yücel and M. Açikgöz, "Optical communication infrastructure in new generation mobile networks," Fiber and Integrated Optics, vol. 42, no. 2, pp. 53–92, 2023 , doi: 10.1080/01468030.2023.2186811.

[20] A. S. Almetwali, O. Bayat, M. M. Abdulwahid, and N. B. Mohamadwasel, "Design and analysis of 50 channel by 40 Gbps DWDM-RoF system for 5G communication based on fronthaul scenario," in Proceedings of Third Doctoral Symposium on Computational Intelligence: DoSCI 2022, Singapore: Springer Nature Singapore, 2022, pp. 109–122.